

Nanoscale Advances

Accepted Manuscript

This article can be cited before page numbers have been issued, to do this please use: B. Makiabadi, F. Naderi, M. Zakarianezhad and A. Raessi, *Nanoscale Adv.*, 2026, DOI: 10.1039/D5NA01168J.



This is an Accepted Manuscript, which has been through the Royal Society of Chemistry peer review process and has been accepted for publication.

Accepted Manuscripts are published online shortly after acceptance, before technical editing, formatting and proof reading. Using this free service, authors can make their results available to the community, in citable form, before we publish the edited article. We will replace this Accepted Manuscript with the edited and formatted Advance Article as soon as it is available.

You can find more information about Accepted Manuscripts in the [Information for Authors](#).

Please note that technical editing may introduce minor changes to the text and/or graphics, which may alter content. The journal's standard [Terms & Conditions](#) and the [Ethical guidelines](#) still apply. In no event shall the Royal Society of Chemistry be held responsible for any errors or omissions in this Accepted Manuscript or any consequences arising from the use of any information it contains.

Investigation of cyclic peptides as drug delivery systems for the delivery of the anti-tuberculosis drug pyrazinamide

Batoul Makiabadi^a, Fereshteh Naderi^{b*}, Mohammad Zakarianezhad^c, Aria Raessi^d

^aDepartment of Chemical Engineering, Sirjan University of Technology, Sirjan, Iran

^bDepartment of Chemistry, ShQ.C., Islamic Azad University, Shahr-e Qods, Iran

^cDepartment of Chemistry, Payame Noor University (pnu), P.O.Box 19395-4697, Tehran, Iran

^dFaculty of Medicine, University of Debrecen, 4032 Debrecen, Hungary

Abstract

One of the important goals of drug delivery in the treatment of diseases is to effectively deliver drugs to deep and inaccessible areas of tissues. In recent years, cyclic peptides (CPs) have been used as drug delivery systems due to their high affinity for their targets, stability against degradation, and low toxicity. In this study, the interaction of the anti-tuberculosis drug pyrazinamide (PY) with cyclic decapeptides of glycine, alanine, and serine and their binary alternating sequences was investigated at the M06-2X/6-31G(d,p) level of theory in the gas phase. Interaction energies, structural parameters, topological properties, as well as RDG, ELF, and IGM analyses were used to assess the strength of interactions in the complexes. The electronic properties of cyclic peptides were investigated and compared before and after the complexation process. Based on the findings of this study, cyclic peptides based on binary alternating sequences have a higher tendency to interact with the pyrazinamide molecule. Therefore, the use of a combination of amino acids in cyclic peptides allowed for the rational design of a new material with more favorable properties. These findings provide insights into the development of more effective drugs using cyclic peptides.

Keywords: Cyclic peptides; Anti-tuberculosis drug, Pyrazinamide, Interaction, Density functional theory, Drug delivery

* Corresponding Author: Fereshteh Naderi, Email:fnaderi@iau.ac.ir



Introduction

The delivery of therapeutic drugs to specific cells is a fundamental issue for the treatment of various human diseases, especially infectious, genetic, and cancer diseases. Developing drug delivery systems to penetrate and deliver drugs to target cells is a suitable solution for effective treatment of diseases [1-7]. Drug delivery systems are materials that prevent drug degradation, increase its effectiveness, reduce its side effects, and control its release at the desired site [8-11]. Recently, many studies have been conducted on the various properties of cyclic peptides and their role as drug carriers [12,13]. Cyclic peptides are polypeptide chains formed by the connection of the amino terminus and carboxyl group of the chain, forming cyclic structures. Compared to linear peptides, cyclic peptides show greater potential for biological activities, due to stable shape and state resulting from their cyclic structure [14-17]. Cyclic peptides have a high affinity for binding to target tissue due to their large surface area. Due to their cyclic nature, these structures have less flexibility and more rigidity, and are therefore more stable [18-21]. By changing the number and type of amino acids in cyclic peptides, the properties of cyclic peptides can be modified as drug delivery systems [22-24]. Wang and colleagues investigated the physicochemical properties of various types of cyclic peptides as drug delivery systems [25]. Fakhari and co-workers reported that the cyclic peptides cyclo[(Ser-Ser)₄], cyclo[(Gly-Gly)₄], and cyclo[(Ala-Ala)₄] could be effective carriers for the drug metformin [26]. A theoretical study was conducted on the properties of the cyclooctaglycine as a carrier for the anti-cancer drug penicillamine [27].

Given the global importance of infectious diseases and the need for effective drug delivery, tuberculosis one of the deadliest infectious diseases worldwide [28,29]. The most common types of drugs used to treat tuberculosis are rifampin, pyrazinamide, and streptomycin. Among the drugs used, pyrazinamide (PY) has shown good performance in treating patients with tuberculosis, by reducing side effects (fever, anorexia, liver enlargement, jaundice, and liver failure) and treatment duration [30,31]. However, current treatment methods have limited effectiveness due to poor patient compliance with the drug regimen or due to the presence of drug-resistant tuberculosis. In recent years, studies have been conducted on the delivery of anti-tuberculosis drugs. [32-36]. Research shows that anti-tuberculosis drugs can be encapsulated in liposomes, microparticles, or nanoparticles for controlled entry and release into lung cells [37-



39]. The use of these therapeutic methods in infected animals shows a significant increase in treatment improvement and reduction in complications and tissue damage [40,41]. In addition to lipid-based and polymeric systems, various nanostructures such as carbon nanotubes (CNTs), fullerenes, boron-nitride nanotubes (BNNTs), and cyclic peptides have been widely investigated as carriers for pyrazinamide [31,42-44]. Although CNTs and BNNTs have high mechanical strength and thermal stability, cyclic peptides have often attracted more attention for drug delivery applications due to their biodegradability, low toxicity, and ease of chemical modification through sequence engineering. Cyclic peptides have the ability to precisely tune the chemistry of the internal cavity by changing the amino acid sequence. This ability to tune the sequence is the main motivation for the present study.

Therefore, in this project, the interaction of the anti-tuberculosis drug PY with cyclic decapeptides of glycine, alanine, and serine and their binary alternating sequences was studied. Studying how drugs bind to cyclic peptides could lead to the design of molecules with higher affinity and fewer side effects. In this study, the complexes resulting from the interaction of the PY with a variety of cyclic peptides were investigated. In this regard, structural parameters, interaction energies, atomic charge distribution, energy gap, electrostatic potential levels, charge transfer, and interactions strength were analyzed. This study attempts to answer the fundamental question, "What effect does changing the amino acid sequence in cyclic peptides have on the interaction with the drug pyrazinamide?" Therefore, in this work, we answer this question by systematically changing the CP sequence. By changing the amino acid sequence in cyclic peptides, an understanding of the structure-function relationship can be achieved, which allows for the rational design of drug carriers based on sequence chemistry. These insights are inaccessible when only a single sequence is studied. It is hoped that this study will provide a better understanding of how drugs bind and the role of the cyclic peptide structure, which could lead to the design of drugs with better absorption in the body.

Computational Methods

Density functional theory (DFT) was used to investigate the interaction of the drug PY with a number of cyclic decapeptides made of alanine, glycine, and serine amino acids. All structures were optimized at the M06-2X/6-31G(d,p) level of theory using the Gaussian 09 software package [45]. The counterpoise procedure (CP) [46] was used to correct for basis set



superposition error (BSSE) in the calculation of different binding energies. The interaction energy (ΔE_{ads}) is calculated as:

$$\Delta E_{\text{int}} = E_{(\text{Comp})} - (E_{(\text{PY})} + E_{(\text{CP})}) \quad (1)$$

where, $E_{(\text{Comp})}$ is the total energy of the complex of the drug interacting with the cyclic peptide, $E_{(\text{PY})}$ is the total energy of a drug molecule, and $E_{(\text{CP})}$ is the total energy of cyclic peptide. For all complexes, the molecular descriptors such as the HOMO–LUMO energy gap (E_{gap}), hardness (η), softness (S), electrophilicity index (ω) and the maximum amount of electronic charge (ΔN_{max}) as:

$$E_{\text{gap}} = E_{\text{LUMO}} - E_{\text{HOMO}} \quad (2)$$

$$\eta = (E_{\text{g}})/2 \quad (3)$$

$$S = 1/(2\eta) \quad (4)$$

$$\omega = (\mu^2/2\eta) \quad (5)$$

$$\Delta N_{\text{max}} = -\mu/\eta \quad (6)$$

When two systems A and B approach each other, the amount of charge transfer between them can be written in terms of electrophilicity. Electrophilicity-based charge transfer (ECT) is obtained by:

$$\text{ECT} = (\Delta N_{\text{max}})_A - (\Delta N_{\text{max}})_B \quad (7)$$

that if $\text{ECT} > 0$ then A is an electron acceptor, while if $\text{ECT} < 0$ it is an electron donor [47].

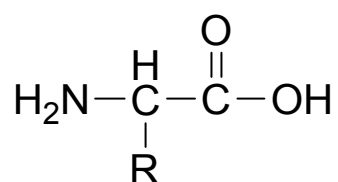
The solvent effect was examined using the M06-2X/6-31G(d,p) level of theory by applying the polarizable continuum model (PCM) [48]. Multiwfn program was used to plot the electron density of states (DOS), the electron localization function (ELF) [49], and independent gradient model (IGM). The reduced density gradient (RDG) plots were rendered by the VMD program [50] based on the outputs of Multiwfn. The NBO and AIM analysis was carried out at the M06-2X/6-31G(d,p) level of theory [51,52].



Results and discussion

Energies and Geometries

DFT calculations were performed to evaluate the interaction of the PY drug with a number of the cyclic peptides. The difference between these cyclic peptides is in the type and alternating sequence of amino acids used in them. In this regard, three types of amino acids were selected, such as alanine, glycine, and serine molecules (Scheme 1).



Amino acid	R
Glycine (G)	H
Alanine (A)	CH ₃
Serine (S)	CH ₂ OH

Scheme 1. The linear structure of the amino acids Glycine, Alanine, and Serine

In the first stage, cyclic peptides composed of one type of amino acid were designed. Using 10 molecules of each, cyclic structures CP_{X-X} (X=S, G, and A) were constructed and named as CP_{G-G}, CP_{A-A}, and CP_{S-S} (See Figure 1).

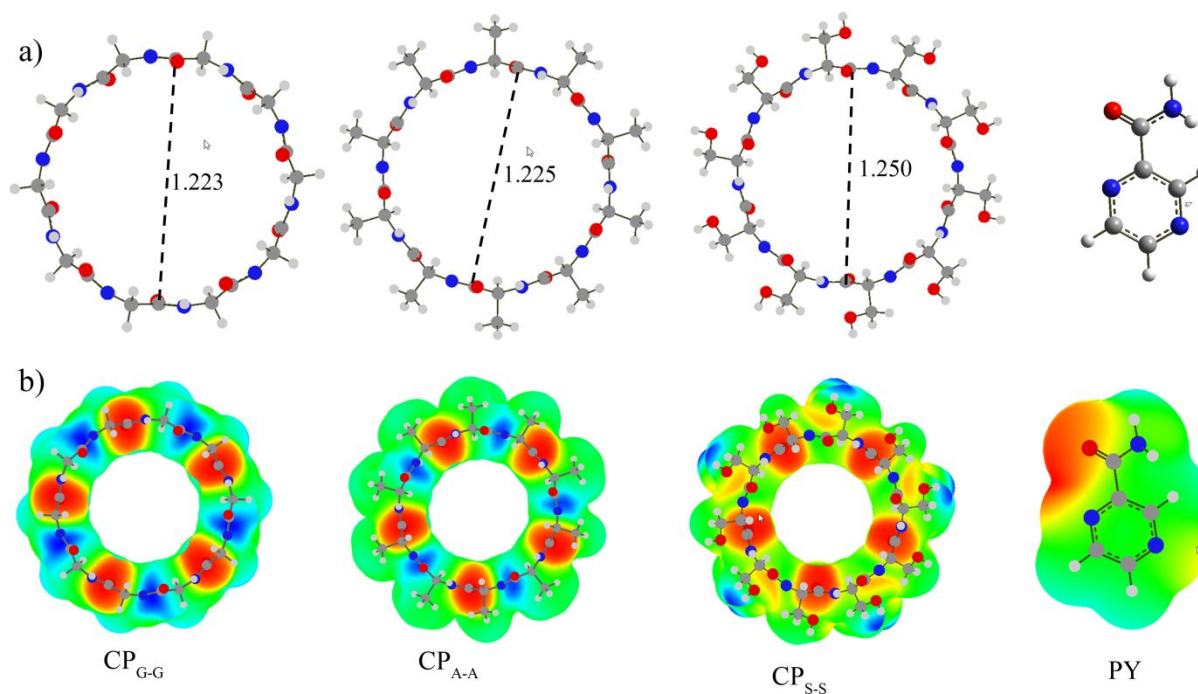


Figure 1. a) The optimized structures, b) the molecular electrostatic potential surface maps for CP_{G-G}, CP_{A-A}, CP_{S-S}, and PY structures.

As seen in the optimized structures, the oxygen atoms of the ketone groups are located alternately up and down of the cyclic peptides. It is observed that the length of C=O, C-C, and C-N bonds increases with the change of R group from hydrogen to methanol. Therefore, it is observed that the length of C-N bonds depends on the R group. The ring diameter from the carbon of the carbonyl group to the carbon of the opposite carbonyl group in CP_{G-G}, CP_{A-A}, and CP_{S-S} is 1.223, 1.225, 1.250 Å, respectively. MESP (The molecular electrostatic potential surface) maps were drawn for the drug and different cyclic peptides (Figure 1). These maps were used to identify suitable sites on the drug and cyclic peptide for interaction with each other. In these color maps, red, blue, and green colors correspond to areas with negative, positive, and zero electrostatic potential, respectively. As can be seen, the oxygen atoms of the drug and the cyclic peptides have negative ESP, while the hydrogen atoms connected to N atoms have positive MESP. Therefore, the negative charges were placed on O atoms, while the positive charges were placed on H atoms. In CP_{S-S}, CP_{G-G}, CP_{A-A}, and PY structures, the average electrostatic potential values (ESP) on the local surface of the O atom of the C=O group is observed with values of -19.8, -22.5, -31.5, and -32.7 kcal/mol, respectively. Therefore, these sites are susceptible to electrophilic attack. In contrast, the average of ESP on the local surface of hydrogen atoms is positive, and thus nucleophilic reagents tend to be attracted to these sites.

In the first step, the DFT calculations were performed to evaluate the interaction of the PY drug with CP_{S-S}, CP_{G-G}, and CP_{A-A} cyclic peptides. The most stable structures, named CP_{S-S}/PY, CP_{G-G}/PY, and CP_{A-A}/PY complexes (See Figure 2). Two types of hydrogen bonds, O...H and N...H, are observed in these complexes.



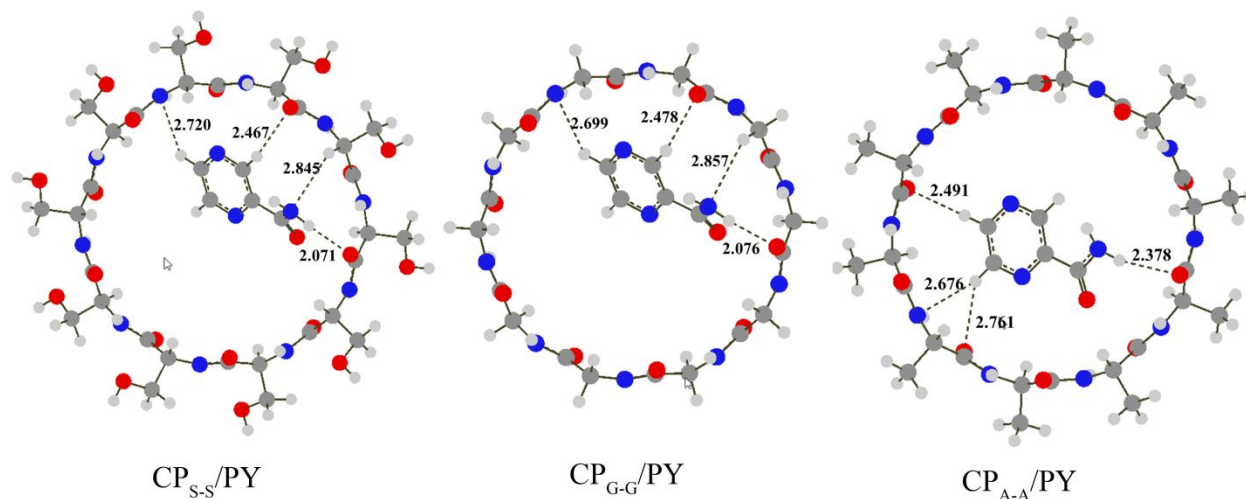


Figure 2. The optimized structures for CP_{X-X}/PY complexes at M06-2X/6-31G(d,p) level of theory

Analysis of structural parameters in CP_{S-S}/PY and CP_{G-G}/PY complexes shows that in the interaction between the drug and the cyclic peptide, two O...H hydrogen bonds and two N...H hydrogen bonds are formed, while in the CP_{A-A}/PY complex, three O...H hydrogen bonds and one H...N hydrogen bond are observed. Hydrogen bonds play important roles in biological systems [53-55]. In the CP_{X-X}/PY complexes, the lengths of the O...H hydrogen bonds are shorter than the N...H hydrogen bonds. These data suggest that O...H hydrogen bonding interactions are stronger than N...H interactions. On the other hand, the O...H hydrogen bond distances in the CP_{S-S}/PY complex are shorter than those in the CP_{G-G}/PY and CP_{A-A}/PY complexes. It is predicted that the O...H hydrogen bonding interactions in the CP_{S-S}/PY complex are stronger than the CP_{G-G}/PY and CP_{A-A}/PY complexes.

Studies show that the orientation of functional groups affects the spatial structure, stability, biological activity, and physicochemical properties of cyclic peptides. Therefore, the sequence of amino acids in the structure of cyclic peptides is of particular importance. To investigate this issue, the cyclic structures CP_{X-Y}/PY ($X=S, G, A$ and $Y=S, G, A, X \neq Y$) were considered. In these structures, the amino acids serine, glycine, and alanine were alternately substituted in CP_{X-X}/PY complexes. The resulting structures were named CP_{S-A}/PY , CP_{S-G}/PY , CP_{G-S}/PY , CP_{G-A}/PY , CP_{A-G}/PY , CP_{A-S}/PY , CP_{S-S}/PY , CP_{G-G}/PY , and CP_{A-A}/PY complexes. The CP_{X-Y}/PY optimized complexes at the M06-2X/6-31G(d,p) level of theory are shown in Figure 3.



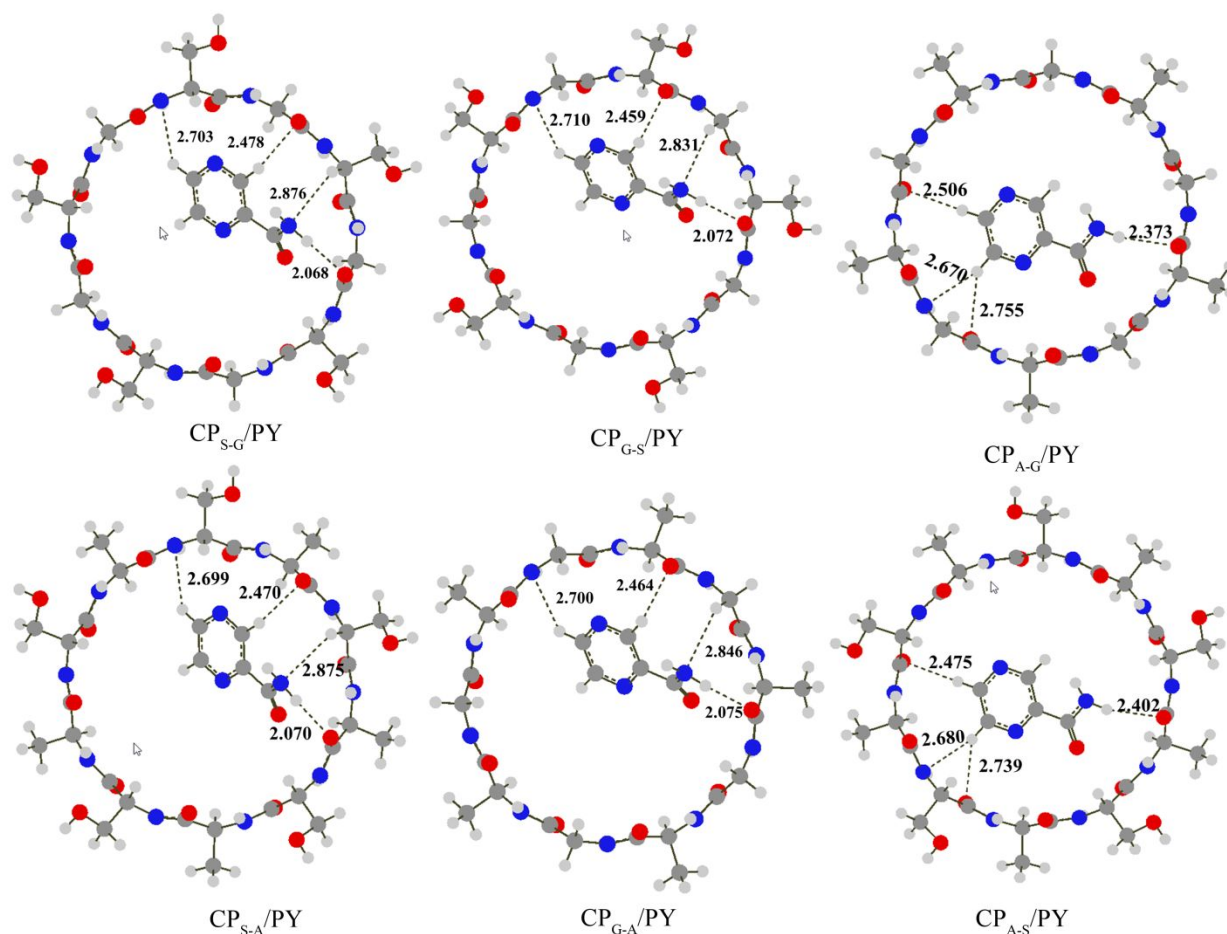


Figure 3. The optimized structures for CP_{X-Y}/PY complexes at M06-2X/6-31G(d,p) level of theory

The number and type of hydrogen bonds observed in CP_{X-Y}/PY complexes are similar to those in CP_{X-X}/PY complexes. Also, in these complexes, the drug is closer to the cyclic peptide from the NH_2CO side. The shortest hydrogen bond distance is 2.068 Å in CP_{S-G}/PY , 2.070 Å in CP_{S-A}/PY , 2.072 Å in CP_{G-S}/PY , 2.075 Å in CP_{G-A}/PY , 2.373 Å in CP_{A-S}/PY and 2.402 Å in CP_{A-G}/PY . This distance appears (O...H hydrogen bond) to be shorter and stronger in CP_{X-Y}/PY complexes than in CP_{X-X}/PY complexes.

The interaction energies (ΔE_{int}) for CP_{X-X}/PY and CP_{X-Y}/PY complexes at two theoretical levels have been summarized in Table 1. Based on the Table 1, the relative stability of complexes decreases in the order $CP_{S-G}/PY > CP_{S-A}/PY > CP_{G-S}/PY > CP_{G-A}/PY > CP_{A-G}/PY > CP_{A-S}/PY > CP_{S-S}/PY > CP_{G-G}/PY > CP_{A-A}/PY$. The results show that the ΔE_{int} values for CP_{X-Y}/PY complexes are more than those for CP_{X-X}/PY complexes. Therefore, structures with more



negative interaction energies are more stable. Also, the type and sequence of amino acids in cyclic peptides affect their stability. According to the results obtained, it can be concluded that CP_{X-Y}/PY structures are more stable than CP_{X-X}/PY complexes. It can be concluded that CP_{X-Y}/PY complexes have a higher affinity for drug interaction than CP_{X-X}/PY complexes. The interaction energy results show that the stability order of the complexes remained unchanged by changing the basis set.

Table 1 The interaction energies (ΔE_{int} /kJmol⁻¹), the recovery time (τ), charge transfer, and the hydrogen bonds energy (E_{HB} , kcal/mol) for all complexes

Structure	ΔE_{int}	$\Delta E_{\text{int}}^{\text{bsse}}$	$\tau(\text{s})$	CT(e)	E_{HB}
CP _{S-S} /PY	-88.74 ^a (-78.50) ^b	-63.04	3.1*10 ³	-0.00004	0.185
CP _{G-G} /PY	-43.64(-20.56)	-28.22	4.1*10 ⁻⁵	-0.00180	0.180
CP _{A-A} /PY	-18.52(-16.03)	-5.53	1.7*10 ⁻⁹	-0.00840	0.104
CP _{S-G} /PY	-100.80 (-95.58)	-69.88	3.8*10 ⁵	-0.00186	0.195
CP _{S-A} /PY	-90.29 (-89.41)	-59.63	5.2*10 ³	-0.00008	0.189
CP _{G-S} /PY	-88.84 (-86.32)	-57.96	3.5*10 ³	-0.00192	0.187
CP _{G-A} /PY	-88.31 (-79.05)	-57.45	2.4*10 ³	-0.00188	0.184
CP _{A-G} /PY	-68.65 (-62.10)	-42.59	0.1*10 ¹	-0.0094	0.102
CP _{A-S} /PY	-67.63 (-60.75)	-41.70	6.7*10 ²	-0.00879	0.072

a: Interaction energies at the M06-2X/6-31G(d,p) level of theory

b: Interaction energies at the M06-2X/6-311++G(d,p) level of theory

The Espinosa-Molins-Lecomte (EML) equation ($E_{\text{HB}}=0.5 \times V(r)$) is a formula used to estimate the energy of hydrogen bonds, where $V(r)$ is the value of local potential energy at the bond critical point [56]. The absolute value of E_{HB} ($|E_{\text{HB}}|$) for the shortest hydrogen bond (O...H) is reported in Table 1. The $E_{\text{HB}}(|E_{\text{HB}}|)$ value depends on the length of the hydrogen bond, so the shorter bonds have more ($|E_{\text{HB}}|$) and vice versa. In CP_{X-Y}/PY complexes, the absolute value of $E_{\text{HB}}(|E_{\text{HB}}|)$ related to O...H hydrogen bond is greater than that of CP_{X-X}/PY complexes. This result is consistent with the shorter and stronger O...H interaction in CP_{X-Y}/PY complexes than in CP_{X-X}/PY complexes. The recovery time (τ) is a critical parameter for gas sensors and drug delivery systems [57]. The term “recovery time” refers to the time required for a drug molecule to dissociate from the substrate surface. The recovery time can be calculated using conventional transition state theory ($\tau = v_0^{-1} \times \exp^{-\Delta E_{\text{int}}/kT}$) [58]. Where ΔE_{int} is the interaction energy, T is the ambient temperature (298.15K), k is the Boltzmann constant, and v_0 is assumed to be 10¹² Hz. We used this formula as a measure to compare the strength of drug binding to the cyclic peptides. The calculated time is used solely to compare the relative strength of interactions in



different structures. High interaction energy indicates a strong interaction between the drug and the cyclic peptide and can lead to a longer recovery time. The results of Table 1 show that the recovery time for CP_{X-Y}/PY complexes is longer than that of CP_{X-X}/PY complexes, which is in agreement with the greater interaction energy of CP_{X-Y}/PY complexes than CP_{X-X}/PY ones. The CP_{X-Y}/PY complexes are more stable than CP_{X-X}/PY complexes and hold the drug for a longer period of time, whereas CP_{X-X}/PY complexes release the drug rapidly, making them suitable for use in sensors. Therefore, the CP_{X-Y}/PY complexes are better for drug delivery due to their longer τ .

The electronic properties of structures

The positions of the highest occupied (HOMO) and lowest unoccupied (LUMO) molecular orbitals determine the electronic properties and reactivity of the structures. HOMO and LUMO orbitals referred to as electron donating and electron accepting orbitals, respectively. The charge distribution of HOMO and LUMO orbitals for monomers and complexes is given in Figures 4 and 5.



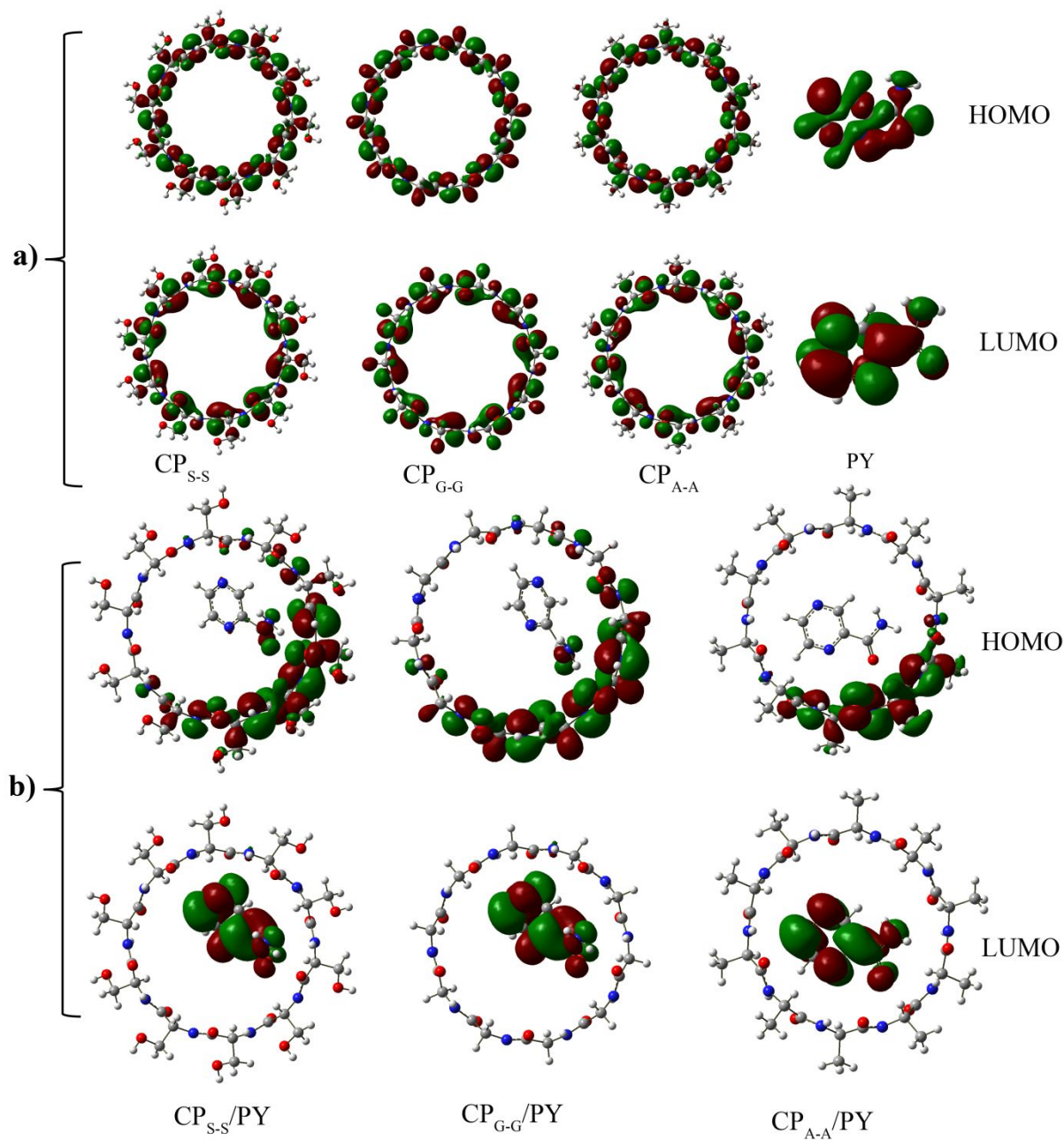


Figure 4. Charge distribution of HOMO and LUMO orbitals for a) monomers and b) the CP_X/PY complexes



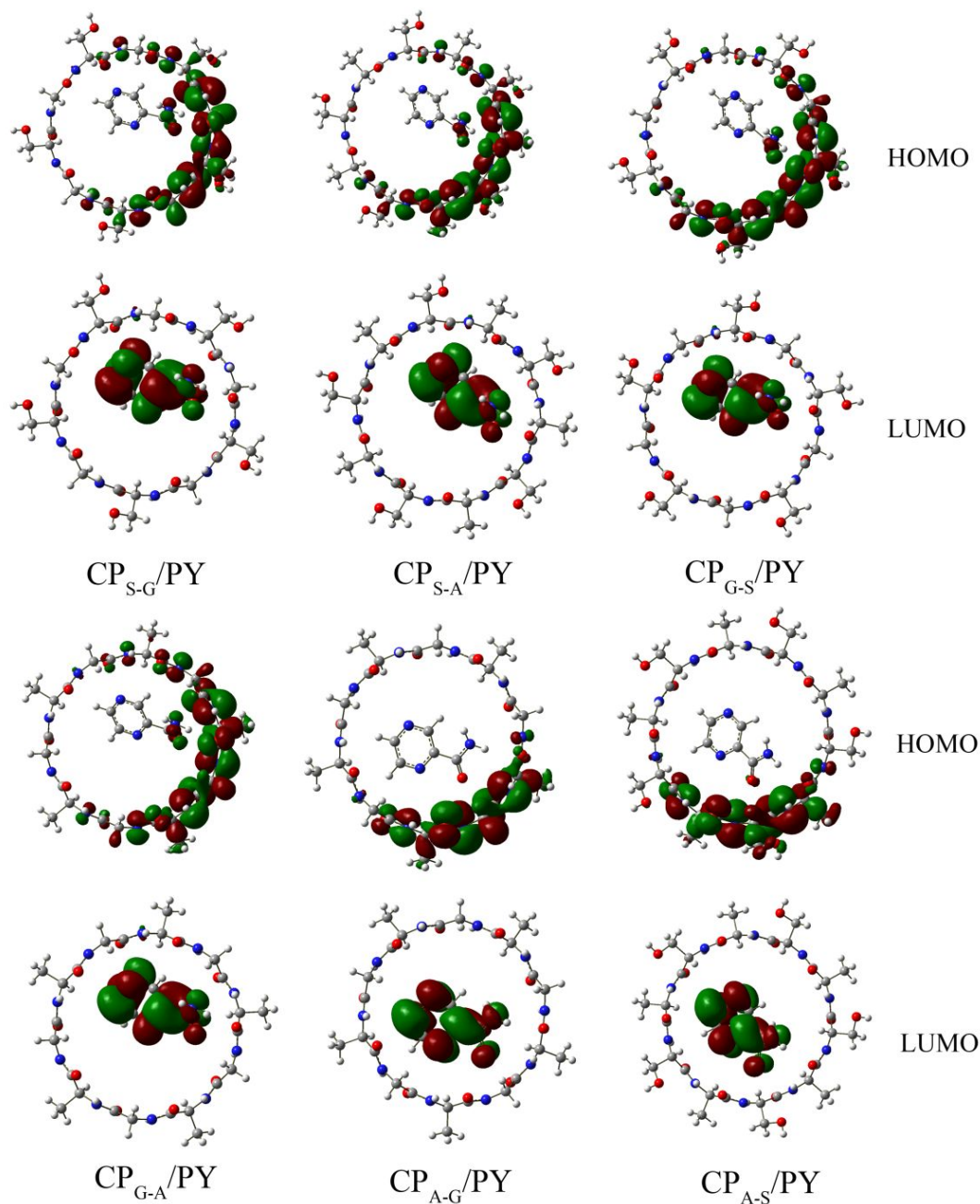


Figure 5. Charge distribution of HOMO and LUMO orbitals for the CP_{X-Y}/PY complexes

As can be seen, in all complexes, the electron density of HOMO is distributed over the cyclic peptide and is mainly placed on the part involved in the interaction, while the LUMO is distributed on the drug. According to Figures 4 and 5, the drug interacts with the HOMO orbitals of the cyclic peptide through its LUMO orbitals. It is predicted that cyclic peptides are more nucleophile, whereas drug molecule is electrophile in nature. The stability of structures depends



on the difference between the energy levels of the HOMO and LUMO orbitals. This difference is called the energy gap. Molecules with higher gap energy are more stable than molecules with lower gap energy. Some of the quantum molecular descriptors for monomers and complexes are given in Table 2.

Table 2 The molecular descriptors for monomers and complexes at the M06-2X/6-31G(d,p) level of theory in the gas phase.

Structure	HOMO(eV)	LUMO(eV)	Eg(eV)	η (eV)	S(eV ⁻¹)	μ (eV)	ω (eV)	ΔN_{\max} (au)	ECT(au)	μ (D)
PY	-8.557	-0.739	7.819	3.909	0.128	-4.648	2.763	0.707		3.41
CPG-G	-8.564	1.363	9.927	4.963	0.101	-3.601	1.306	0.263		0.00
CPA-A	-8.488	1.251	9.739	4.869	0.103	-3.618	1.344	0.276		0.00
CPS-S	-8.080	1.476	9.556	4.778	0.105	-3.302	1.141	0.239		0.00
CPS-A	-8.218	1.274	9.492	4.746	0.105	-3.472	1.270	0.268		1.80
CPS-G	-8.311	1.334	9.645	4.823	0.104	-3.489	1.262	0.262		0.54
CPG-A	-8.523	1.097	9.620	4.810	0.104	-3.713	1.433	0.298		0.42
CP _{G-G} /PY	-8.446	-0.821	7.625	3.812	0.131	-4.634	2.816	0.739	0.476	2.73
CP _{A-A} /PY	-7.880	-0.581	7.299	3.649	0.137	-4.230	2.452	0.672	0.404	3.57
CP _{S-S} /PY	-7.958	-0.297	7.661	3.831	0.131	-4.128	2.224	0.581	0.342	2.45
CP _{S-A} /PY	-8.131	-0.525	7.606	3.803	0.131	-4.328	2.463	0.648	0.380	2.77
CP _{S-G} /PY	-8.174	-0.567	7.607	3.803	0.131	-4.371	2.511	0.660	0.399	2.88
CP _{G-S} /PY	-8.186	-0.542	7.644	3.822	0.131	-4.364	2.492	0.652	0.390	2.92
CP _{G-A} /PY	-8.379	-0.749	7.630	3.815	0.131	-4.564	2.730	0.716	0.418	2.78
CP _{A-G} /PY	-8.132	-0.842	7.290	3.645	0.137	-4.487	2.762	0.758	0.460	3.37
CP _{A-S} /PY	-8.071	-0.771	7.300	3.650	0.137	-4.421	2.677	0.734	0.457	3.37

After the interaction of the PY with cyclic peptides, the HOMO and LUMO states move to lower and higher negative energies, respectively. Due to this change, the energy gap is reduced. This reduction in the energy gap can affect the fluorescence emission of the complexes and aiding in tracking the direction of the drug. The energy gap for CP_{X-Y} structures is lower than that of CP_{X-X} ones. It is predicted that CP_{X-Y}/PY complexes are more reactive than CP_{X-X}/PY complexes, with a greater tendency to interact with drug. The results show that after complexation, the energy gap of CPs decreased, indicating that the interaction of the drug with CPs increases the reactivity of CPs. The energy gap values for complexes are decreased as follows: **CP_{X-X}/PY:** CP_{S-S}/PY > CP_{G-G}/PY > CP_{A-A}/PY; **CP_{X-Y}/PY:** CP_{G-S}/PY > CP_{G-A}/PY > CP_{S-G}/PY > CP_{S-A}/PY > CP_{A-S}/PY > CP_{A-G}/PY. The amount of the energy gap for CP_{A-A}/PY and CP_{S-S}/PY complexes is more than that of their corresponding CP_{X-Y}/PY complexes (CP_{A-S}/PY, CP_{A-G}/PY, CP_{S-A}/PY, CP_{S-G}/PY). Therefore, the reactivity of CP_{A-A}/PY and CP_{S-S}/PY complexes is less than their corresponding CP_{X-Y}/PY complexes. This result is consistent with the lower interaction energy of



CP_{A-A}/PY and CP_{S-S}/PY complexes compared to the corresponding P_{X-Y}/PY complexes. The opposite of this result was observed in the CP_{G-G}/PY complex. For further investigation, the total density of states (TDOS) and projected density of states (PDOS) diagrams for monomers and complexes are shown in Figure 6. According to the plots, the LUMO and HOMO states shift towards more negative and lower values, respectively, which reduces the energy gap of CPs after interaction with the drug. In these diagrams, CPs and PY have the highest and lowest contributions, respectively.

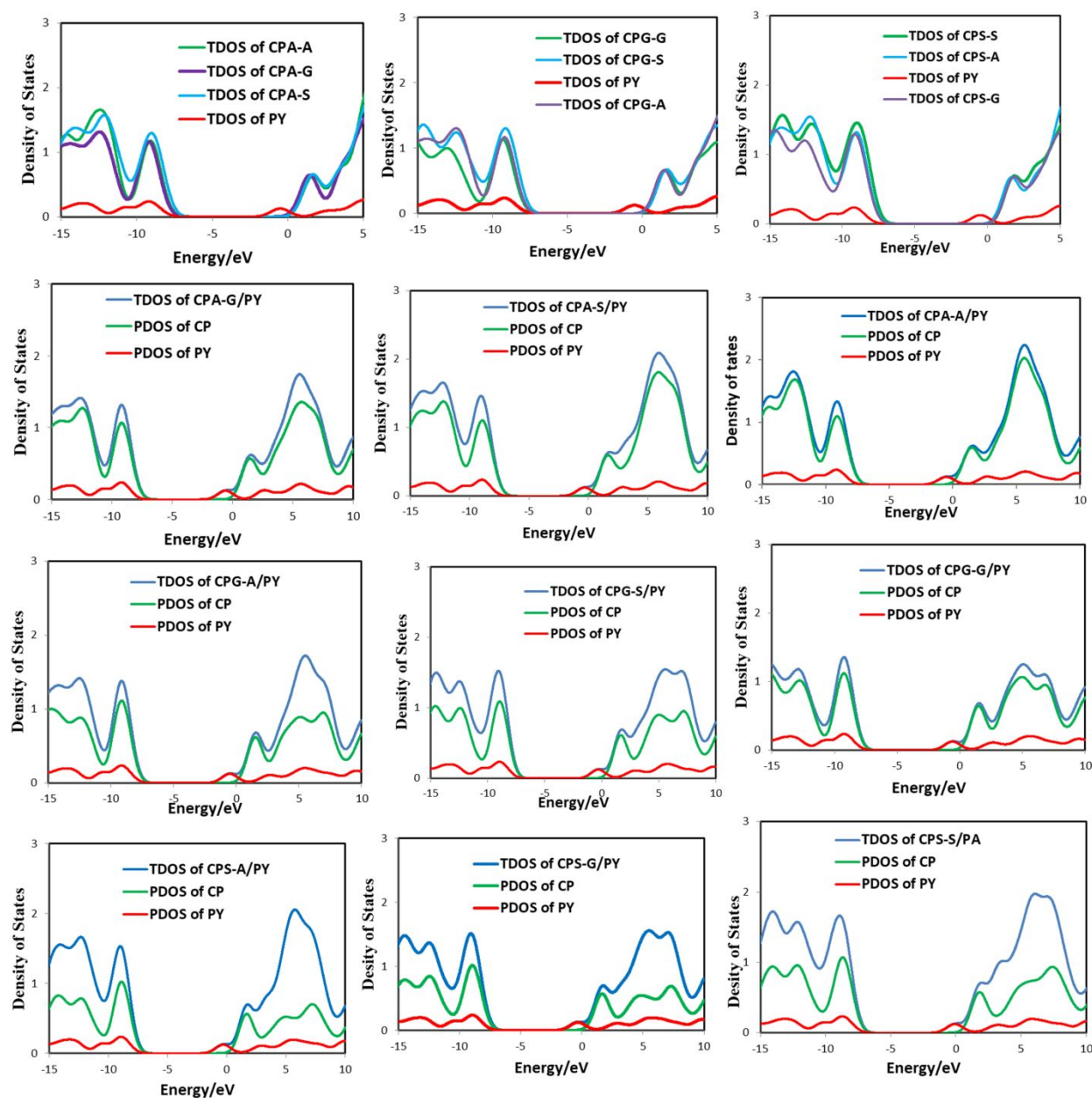


Figure 6. The total and projected density of states for CP_{X-X}/PY and CP_{X-Y}/PY complexes

The reactivity of chemical species could be associated with the molecular descriptors such as electronic chemical potential (μ), hardness (η), softness (S), electrophilicity index (ω), dipole moment (μ), and the maximum charge transfer (ΔN_{\max}) (Table 2). As can be seen, these molecular descriptors changed upon complexation. In CP_{X-X}/PY and CP_{X-Y}/PY complexes, the value of η decreases, whereas the value of S , ω , μ , and ΔN_{\max} increases upon complexation. Comparison of molecular descriptors in all complexes shows that the values of E_g and η for CP_{A-A}/PY and CP_{S-S}/PY complexes is more than their corresponding CP_{X-Y}/PY complexes (CP_{A-S}/PY , CP_{A-G}/PY , CP_{S-A}/PY , CP_{S-G}/PY), in contrast, the values of S , ω , and ΔN_{\max} for CP_{A-A}/PY and CP_{S-S}/PY complexes is less than their corresponding CP_{X-Y}/PY complexes. It is predicted that the affinity of CP_{A-A}/PY and CP_{S-S}/PY complexes to the PY drug is less than that of their corresponding CP_{X-Y}/PY complexes. The opposite of this result was observed in the CP_{G-G}/PY complex. From Table 2, the dipole moment of CPs increases upon complexation. The dipole moment of the CP_{X-Y}/PY complexes is more than that in CP_{X-X}/PY complexes. Therefore, cyclic peptides with alternating sequences show a higher affinity for drug interaction in the gas phase. It is predicted that, in a polar solvent, the solubility of CP_{X-Y}/PY complexes is higher than that of CP_{X-X}/PY complexes.

Solvent Effects

Given the vital role of water in the human body, this substance was chosen as the solvent to study the behavior of CP/PY complexes under conditions similar to the biological environment. The interaction energies (ΔE_{sln}), Gibbs free energies of solvation (ΔG_{solv}^0), the energy gap, electronic chemical potential (μ), hardness (η), softness (S), ΔN_{\max} and dipole moment for the most stable complexes under water solvent are given in Table 3. All calculations were performed at the M06-2X/6-31G(d,p) level of theory. According to the results, the interaction energies (ΔE_{sln}) of complexes have decreased in water solvent. The ΔE_{sln} value for CP_{S-S}/PY complex is lower than that of their corresponding CP_{X-Y}/PY complexes, indicating that in the solution phase, the affinity of CP_{S-A}/PY and CP_{S-G}/PY complexes to the PY drug is higher than that of the CP_{S-S}/PY complex. The stability order of the CP_{X-Y}/PY complexes is almost similar to that of the gas phase. The negative values of ΔG_{solv}^0 show that the solvation process is spontaneous. Therefore,



the solubility of the system is increased upon complexation. The ΔG^0_{Solv} can be separated in to: $\Delta G^0_{\text{Solv}} = \Delta G^0_{\text{Solv,elec}} + \Delta G^0_{\text{Solv, nonelec}}$. From Table 3, the contribution of the electrostatic component of ΔG^0_{Solv} is greater than the non-electrostatic component for complexes. Therefore, the electrostatic interactions between the solvent and the solute can lead to changes in the relative energies of the species in water.

Table 3 The electrostatic ($\Delta G^0_{\text{Solv,elec}}$) and Non-electrostatic ($\Delta G^0_{\text{Solv,nonelec}}$) contributions to the Gibbs free energy of solvation (ΔG^0_{Solv}), the interaction energy in solution (ΔE_{sln}), dipole moment (D), and the molecular descriptors for most stable complexes at the M06-2X/6-31G(d,p) level of theory in the solution phase.

Structure	ΔE_{sln}	ΔG^0_{Solv}	$\Delta G^0_{\text{Solv,elec}}$	$\Delta G^0_{\text{Solv,non-elec}}$	$\mu(\text{D})$	Eg(eV)
CP _{S-S} /PY	-55.97	-62.48	-83.5	21.02	3.25	7.858
CP _{S-G} /PY	-78.64	-80.73	-96.61	15.88	7.83	7.728
CP _{S-A} /PY	-62.59	-77.71	-97.62	19.91	5.23	7.724
Structure	$\eta(\text{eV})$	S(eV ⁻¹)	$\mu(\text{eV})$	$\omega(\text{eV})$	$\Delta N_{\text{max}}(\text{au})$	
CP _{S-S} /PY	3.929	0.12726	-4.622	2.719	0.692	
CP _{S-G} /PY	3.864	0.12940	-4.605	2.745	0.710	
CP _{S-A} /PY	3.862	0.12946	-4.608	2.749	0.712	

The value of the dipole moment of complexes in the solution phase shows that the dipole moment of the complexes has increased in going from the gas phase to the solution phase. Therefore, the dipole moment of the complexes increases after dissolution. Examination of the results in Table 3 show that the values of Eg and η for CP_{S-A}/PY and CP_{S-G}/PY complexes is less than CP_{S-S}/PY complex, in contrast, the values of S, ω , and ΔN_{max} for CP_{S-A}/PY and CP_{S-G}/PY complexes is more than CP_{S-S}/PY complex. These results are consistent with the gas phase results. Comparison of the solution-phase data shows that in the CP_{S-S}/PY complex, the energy gap, chemical hardness, chemical potential, electrophilicity index, and ΔN_{max} decreased, while softness increased compared to the gas phase. The opposite trend is observed for the CP_{S-A}/PY and CP_{S-G}/PY complexes.

NBO, AIM, ELF, and RDG analysis

In this work, the electron density transfers are investigated using NBO analysis. The results of the NBO analysis at M06-2X/6-31G(d,p) level of theory are reported in Table 1. Non-covalent interactions between species lead to changes in the sum of their atomic charges. After



complexation, the sum of the atomic charges of CPs and drug atoms changes, indicating that charge transfer (CT) occurs between the PY and CP. The charge transfer can be defined as the sum of atomic charges on a drug. The results show that, in all complexes, the charge transfers occur from the CP to PY. The amount of charge transfer in CP_{X-Y}/PY complexes is more than that of CP_{X-X}/PY complexes. This result is consistent with the higher interaction energy and higher affinity of CP_{X-Y}/PY complexes with the drug than $CP_{X-X}/BNNT$ complexes. Investigations show that an alternating sequence of amino acids increases the charge transfer between the drug and the CP. In the CP_{X-Y}/PY complexes, strong interactions between the drug and the cyclic peptide enhance the charge transfer from the cyclic peptide to the drug. In each class of CP_{X-Y}/PY structures, a quantitative correlation is observed between the interaction energy and the charge transfer rate, such that structures with higher interaction energy show higher charge transfer rates. This trend indicates that increasing the interaction strength enhances electron redistribution, which is expected to improve the stability of the drug-carrier complex. Small values of charge transfer for non-covalent interactions indicate that no covalent bond is formed and the reversible nature of the carrier-drug interaction is maintained. Also, the data trend shows that a small increase in charge transfer is positively correlated with the enhancement of the interaction energy (ΔE_{int}).

The quantum theory of atoms in molecules (QTAIM) was used to determine the nature of interactions. In this study, to determine the nature of the interactions between cyclic peptides and the PY drug, AIM analysis was performed at M06-2X/6-31G(d,p) level of theory. The molecular graphs indicating the bond critical points (BCPs) and bond paths for CP_{X-X}/PY complexes are shown in Figure 7. In all complexes, the molecular graphs represent additional critical points in the intermolecular regions.

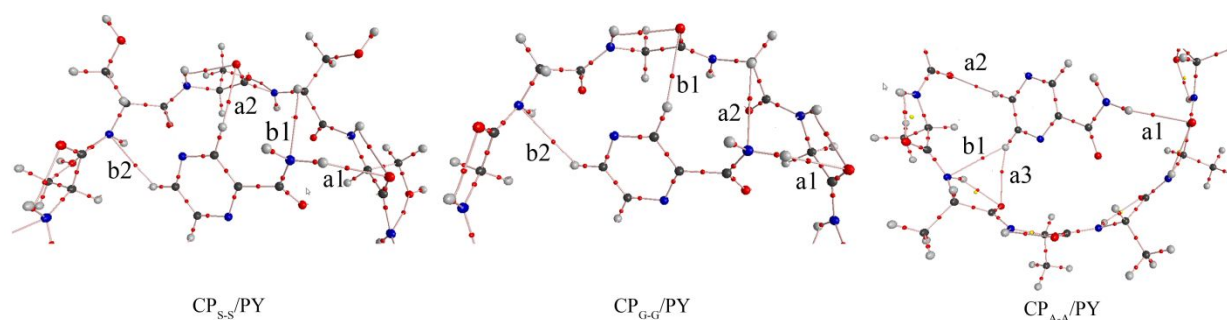


Figure 7. Molecular graphs for CP_{X-X}/PY complexes at M06-2X/6-31G(d,p) level of theory



The values of electron density, $\rho(r)$, the electron density Laplacian, $\nabla^2\rho(r)$, total electronic energy density, $H(r)$, at O...H and N...H bond critical points (BCPs) of complexes are reported in Table 4.

Table 4 Calculated BCPs data (au) for CP_{X-X}/PY and CP_{X-Y}/PY complexes at M06-2X/6-31G(d,p) level of theory.

Bond	$\rho(r)$	$\nabla^2\rho(r)$	$H(r)$	$\rho(r)$	$\nabla^2\rho(r)$	$H(r)$	$\rho(r)$	$\nabla^2\rho(r)$	$H(r)$	
		CP_{A-A}/PY			CP_{G-G}/PY			CP_{S-S}/PY		
(O...H) _{a1}	0.0105	0.0336	0.0077	0.0192	0.0583	0.0157	0.0194	0.0594	0.0160	
(O...H) _{a2}	0.0096	0.0304	0.0065	0.0100	0.0327	0.0068	0.0102	0.0331	0.0070	
(O...H) _{a3}	0.0058	0.0204	0.0034	-	-	-	-	-	-	
(N...H) _{b1}	0.0081	0.0248	0.0048	0.0063	0.0197	0.0035	0.0065	0.0199	0.0036	
(N...H) _{b2}	-	-	-	0.0081	0.0256	0.0049	0.0077	0.0248	0.0046	
		CP_{A-G}/PY			CP_{G-A}/PY			CP_{S-G}/PY		
(O...H) _{a1}	0.0106	-0.0085	0.0078	0.0195	0.0599	0.0161	0.0197	0.0599	0.0162	
(O...H) _{a2}	0.0094	-0.0074	0.0063	0.0099	0.0325	0.0067	0.0104	0.0339	0.0072	
(O...H) _{a3}	0.0059	-0.0052	0.0035	-	-	-	-	-	-	
(N...H) _{b1}	0.0082	-0.0063	0.0049	0.0061	0.0189	0.0033	0.0069	0.0213	0.0038	
(N...H) _{b2}	-	-	-	0.0079	0.0251	0.0048	0.0079	0.0254	0.0047	
		CP_{A-S}/PY			CP_{G-S}/PY			CP_{S-A}/PY		
(O...H) _{a1}	0.011	0.03516	0.00833	0.0195	0.0588	0.0159	0.0196	0.0588	0.0159	
(O...H) _{a2}	0.009	0.02963	0.00622	0.0104	0.0336	0.0072	0.0101	0.033	0.0069	
(O...H) _{a3}	0.005	0.0194	0.00316	-	-	-	-	-	-	
(N...H) _{b1}	0.008	0.0244	0.00482	0.0067	0.0205	0.0037	0.0061	0.0189	0.0033	
(N...H) _{b2}	-	-	-	0.0079	0.0253	0.0047	0.008	0.0255	0.0048	

The results show that the electron densities at O...H interactions are greater than those of at N...H ones that are in agreement with the smaller O...H distance in comparison with the N...H ones. Thus, it is predicted that in all complexes, O...H interactions are stronger than N...H ones. Comparison of $\rho(r)$ values shows that the $\rho(r)$ value corresponding to the shortest interaction (O...H)_a in CP_{X-Y}/PY complexes is higher than its value in CP_{X-X}/PY complexes. This result is consistent with the shorter distance of this interaction in CP_{X-Y}/PY complexes compared to CP_{X-X}/PY complexes. The values of $\nabla^2\rho(r)$ and $H(r)$ at hydrogen bond critical points in all the complexes are positive. Therefore, values of $\nabla^2\rho(r)$ and $H(r)$ indicate that all H-bonds have electrostatic nature.



The RGD analysis is used to investigate the strength of interactions in intermolecular regions. The reduced density gradient (RDG) is a scalar field of the electron density (ρ) that can be defined as:

$$\text{RDG}(r) = \frac{|\nabla\rho(r)|}{2(3\pi^2)\rho(r)^{4/3}} \quad (9)$$

where, $\rho(r)$ and $\nabla\rho(r)$ are the electron density and its first derivative, respectively [59]. In these diagrams, the attractive, van der Waals, and repulsive interactions are marked with blue, green, and red colors, respectively. The RDG plots for the optimized complexes are displayed in Figure 8.

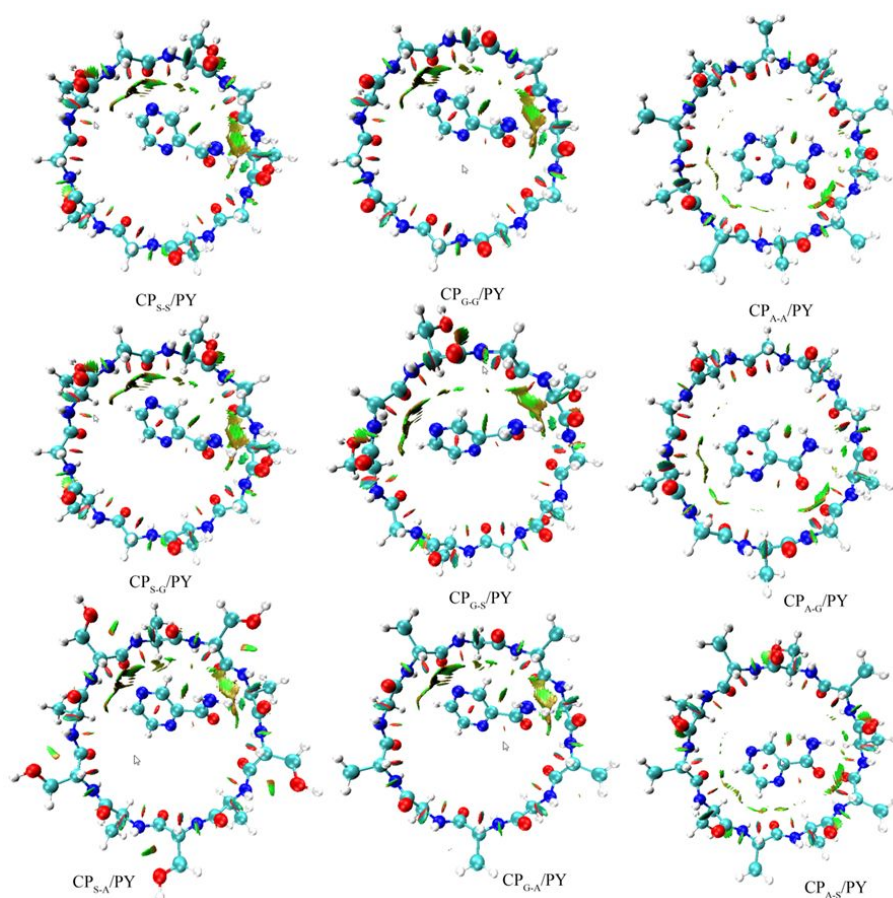


Figure 8. The RDG map for the optimized complexes



In RDG plots, the areas between drug and the cyclic peptides are mainly marked with green and brown color isosurfaces, which show that the interactions are the type of non-covalent and vdW. Van der Waals interactions refer to weak non-covalent interactions, including hydrogen bonding, with electrostatic dominance. These non-covalent interactions are confirmed by the independent gradient model (IGM) and δg descriptive function. The IGM analysis allows separating the δg as δg^{inter} and δg^{intra} , which solely reflect the contribution to δg due to inter-fragment (non-covalent) and intra-fragment (covalent) interactions, respectively. According to the IGM- δg scattered map of different complexes, inter-fragment or intra-fragment interactions are shown in Figure 9. The red and black scattered points correspond to δg^{inter} and δg^{intra} fragments interactions, respectively. In the region where $\text{sign}(\lambda_2)\rho$ is about -0.04, it can be seen that the δg^{inter} has a remarkable peak (With a height of nearly 0.05), which implies the presence of hydrogen bonds.



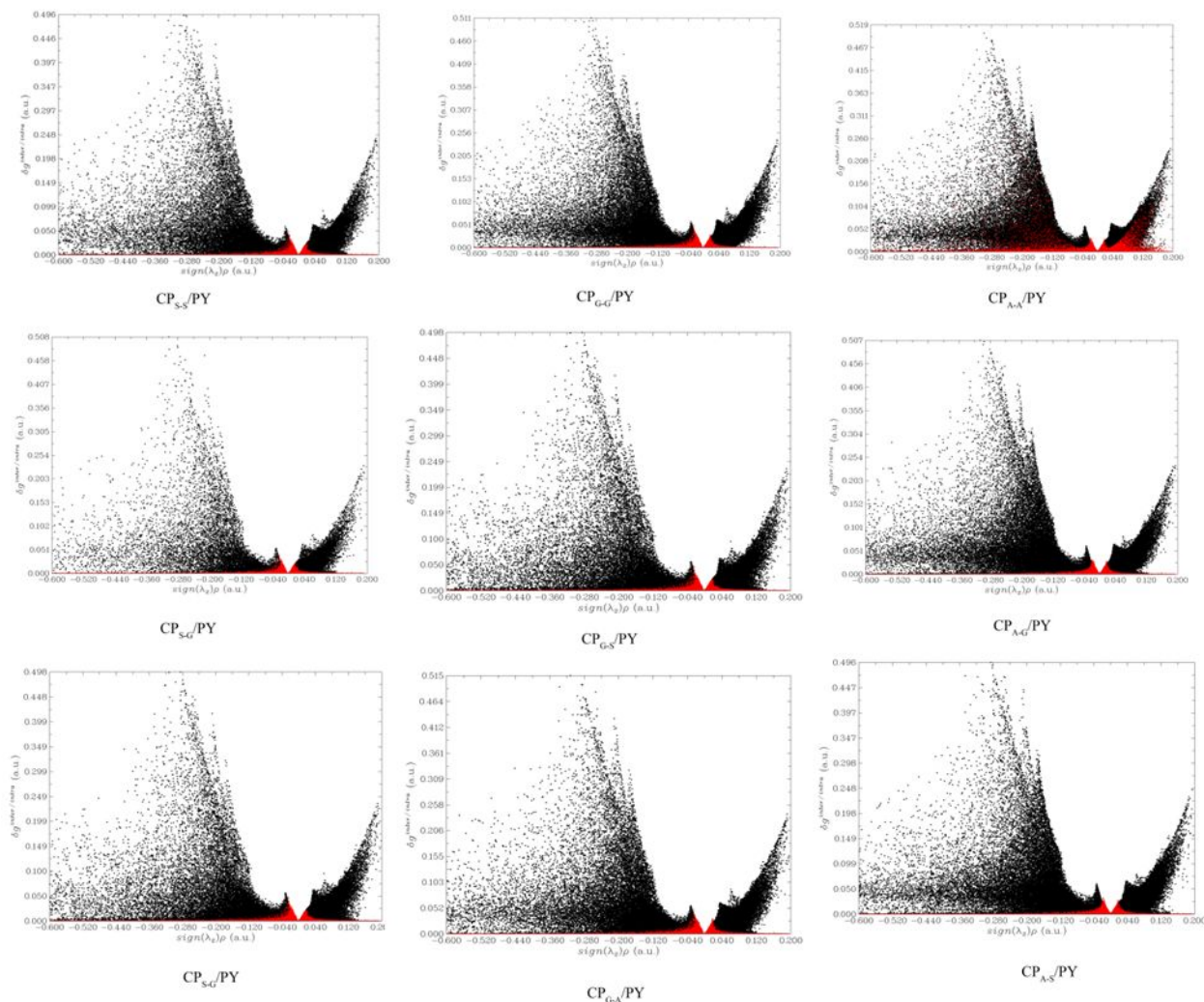


Figure 9. Independent Gradient Model (IGM) of PY on CP_{X-X}/PY and CP_{X-Y}/PY complexes.

In the continuation of work, ELF (electron localization function) maps for all complexes were plotted using Multiwfn and are shown in Figure 10.



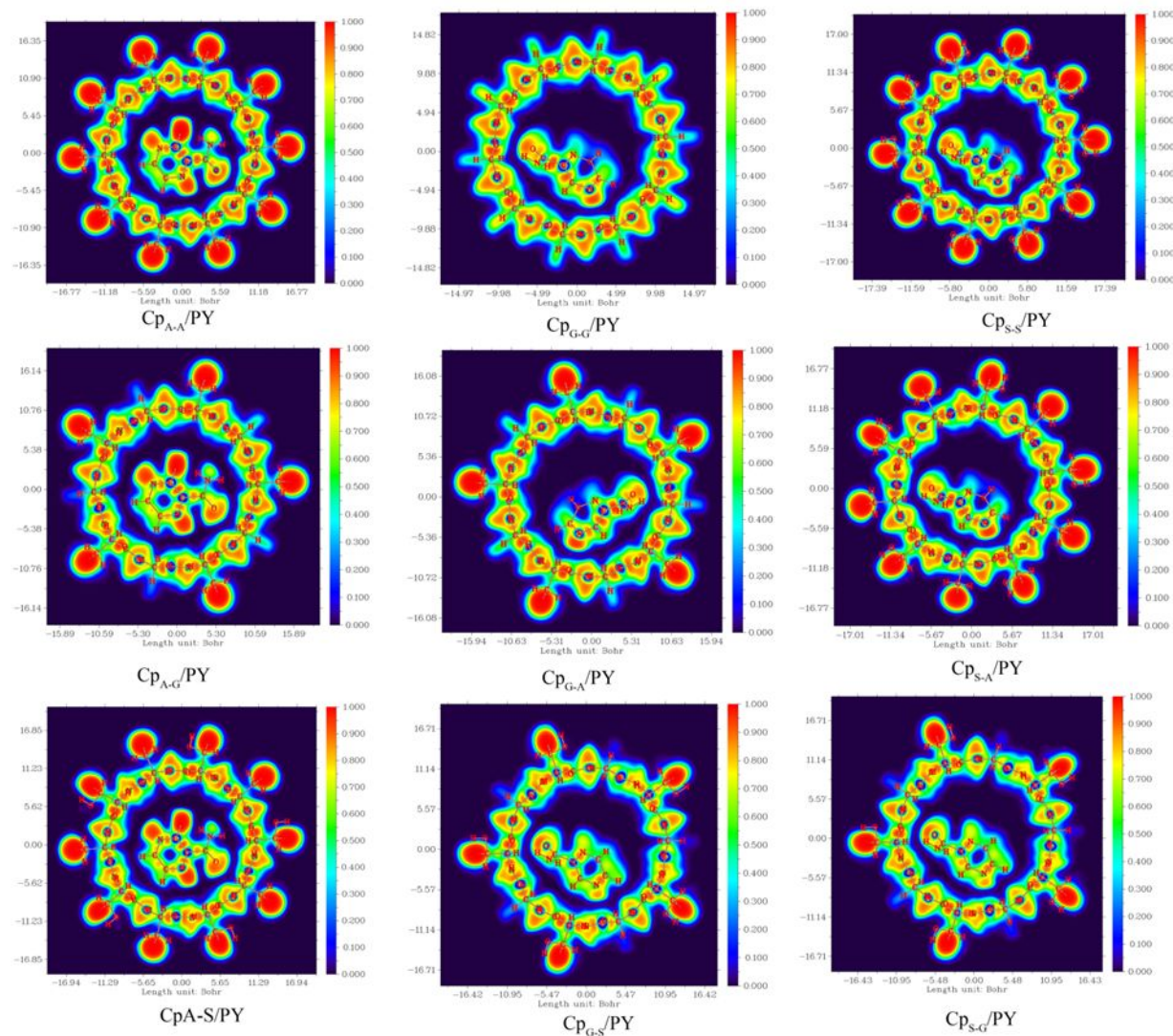


Figure 10. ELF maps of the interaction of the PY drug with cyclic peptides

This map represents the homogeneous Jellium-like electron gas model; the values are normalized between 0.0 and 1.0. The red regions indicate extreme localization (value 1.0). The green regions indicate a free electron gas behavior (value 0.5), and the blue regions indicate non-localization (value 0.0). The presence of these colored regions between the drug and the cyclic peptide indicates electron localization between the drug and the cyclic peptide. Figure 10 shows relatively strong electron localization between the NH_2CO group of drug and the cyclic peptide ring (yellow color). It indicates that the interactions are stronger in this region.



The results of this study provide an electronic and structural basis for understanding the effect of amino acid sequence in cyclic peptides on the interaction with pyrazinamide. Therefore, this is the first step towards the rational design of drug carriers. In the next step, other properties of the structures, including thermal stability, toxicity, drug release, membrane permeability, and bioavailability, should be evaluated in in vivo studies.

Conclusion

This research focuses on investigating the interaction of anti-tuberculosis drug PY with the cyclic decapeptides of Glycine(G), Alanine(A), and Serine(S) and their binary alternating sequences at the M06-2X/6-31G(d,p) level of theory in the gas and solution phases. So we are dealing with two types of complexes CP_{X-X}/PY (CP_{S-S}/PY , CP_{G-G}/PY , CP_{A-A}/PY) and CP_{X-Y}/PY (CP_{S-A}/PY , CP_{S-G}/PY , CP_{G-S}/PY , CP_{G-A}/PY , CP_{A-G}/PY , CP_{A-S}/PY). In the obtained complexes, two types of hydrogen bonds, O...H and N...H, were observed. It seems that hydrogen bonds formed between the drug and cyclic peptides play an important role in the stability of the complexes. Comparison of the two types of hydrogen bonds in the complexes shows that the O...H hydrogen bonds are shorter than the N...H bonds. On the other hand, the O...H interactions observed in CP_{X-Y}/PY complexes are shorter than those in CP_{X-X}/PY complexes. Hence, in CP_{X-Y}/PY complexes, the absolute value of $E_{HB}(|E_{HB}|)$ related to O...H hydrogen bond is greater than that of CP_{X-X}/PY complexes. Examination of the energy results shows that the affinity of CP_{X-Y}/PY complexes for drug interaction is higher than that of CP_{X-X}/PY complexes. Thus, it is predicted the interactions in CP_{X-Y}/PY complexes be stronger than CP_{X-X}/PY complexes. The hydrogen interactions in the complexes are of the Van der Waals type. Therefore, PY drug can physically interact with the cyclic peptides. The value of the dipole moment for CP_{X-Y}/PY complexes is more than CP_{X-X}/PY complexes, indicating that the polarity of CP_{X-Y}/PY complexes is more than CP_{X-X}/PY complexes. The energy gap values for the CP_{A-A}/PY and CP_{S-S}/PY complexes are more than those for the CP_{X-Y}/PY complexes. Therefore, the affinity of CP_{A-A}/PY and CP_{S-S}/PY complexes to the PY drug is less than that of their corresponding CP_{X-Y}/PY complexes. This result is also observed for the most stable complex in the solution phase. The dipole moment value of the complexes in the solution phase has increased compared to the gas phase. In all complexes, the charge transfer takes place from the cyclic peptide to the drug. The amount of charge transfer in CP_{X-Y}/PY complexes is more than



CP_{X-X}/PY. Structures with higher interaction energy show higher charge transfer rates. Based on the AIM analysis, the electron density $\rho(r)$ at O...H BCPs for CP_{X-Y}/PY complexes is more than that of the CP_{X-X}/PY complexes, which corresponds to the higher interaction energy in these structures. This result is in agreement with the shorter O...H hydrogen bond distances in the CP_{X-Y}/PY complexes compared to CP_{X-X}/PY ones. The nature of the O...H and N...H interactions in all complexes is electrostatic. Finally, the alternating sequence of amino acids in cyclic peptides increases the stability of the structures and improves their properties. Hence, the affinity of CP_{X-Y}/PY complexes for interaction with PA is stronger than that of CP_{X-X}/PY complexes.

Conflicts of interest

All authors declare that they have no conflicts of interest.

Data Availability Statement:

Data available on request from the authors.

References

- (1) Jamróży, M.; Kudłacik-Kramarczyk, S.; Drabczyk, A.; Krzan, M. Advanced drug carriers: a review of selected protein, polysaccharide, and lipid drug delivery platforms. *Int. J. Mol. Sci.* **2024**, *25* (2), 786.
- (2) Khudhair, A. M.; Ahmed, A. B.; Ajeel, F. N. Computational Investigation of 6-Thioguanine Adsorption on Armchair Graphene Nanoribbons for Targeted Drug Delivery: Orientation-Dependent Stability, Electronic Structure, and Delivery Efficiency, *J. Phys. Chem. C.* **2025**, *129*, 16593–16603.
- (3) Khudhair, A. M.; Dhouib, I.; Ahmed, A. B.; Ajeel, F. N.; Khemakhem, B. DFT-based insights into cisplatin drug adsorption on transition metal dichalcogenides: toward targeted drug delivery systems, *Chinese Journal of Physics.* **2025**, *97*, 827–838.



- (4) Naderi, F.; Veryazov, V. Multiconfigurational Study of the Electronic Structure of Negatively Charged Fullerenes. *J. Chem.* **2017**, *11*, 30–36.
- (5) Khudhair, A. M.; Dhouib, I.; Ajeel, F. N.; Ahmed, A. B.; Khemakhem, B. A Novel $A_{18}N_8$ and B_8N_8 Nanoring Monolayer for Sensing and Drug Delivery of Cisplatin and Nitrosourea Anticancer Drugs: A DFT Insight, *J. Inorg. Organomet. Polym. Mater.* **2025**, *35*, 7593–7606
- (6) Ghasemi, A. S.; Makiabadi, B.; Zakarianezhad, M.; Soltani, A.; Ashrafi, F.; Mashhadban, F. Experimental and theoretical studies of the interaction of Penicillamine with SWCNT (6, 0) as a drug delivery system. *Inorg. Nano-Met. Chem.* **2024**, *54* (6), 525–533.
- (7) Makiabadi, B.; Zakarianezhad, M.; Zeydabadi, E. The role of hydrogen bonds on the stability of anticancer drug compounds TG/uracil, TG/5-fluorouracil and TG/gimeracil. *Struc. Chem.* **2023**, *34* (3), 755–767.
- (8) Naderi, F.; Veryazov, V. The electronic structure of negatively charged fullerenes: From monomers to dimers. *Comput. Methods Sci. Eng.* **2017**, *1906* (1), 030024.
- (9) Makiabadi, B.; Naderi, F.; Zakarianezhad, M. Theoretical investigation of Diels–Alder reaction mechanism and regioselectivity with functionalized fullerene derivatives. *J. Chin. Chem. Soc.* **2024**, *71* (12), 1418–1426.
- (10) Bardan, K. H.; Ajeel, F. N.; Mohammed, M. H.; Khudhair, A. M.; Ahmed, A. B. DFT study of adsorption properties of the ammonia on both pristine and Si-doped graphene nanoflakes, *Chem. Phys. Impact.* **2024**, *8*, 100561.
- (11) Khudhair, A. M.; Ahmed, A. B.; Ajeel, F. N.; Mohammed, M. H. Theoretical investigation on the therapeutic applications of C2B and C2O as targeted drug delivery systems for hydroxyurea and 6-thioguanine in cancer treatment, *Nano-Structures&Nano-Objects.* **2024**, *38*, 101135
- (12) Khoshbayan, B.; Morsali, A.; Beyramabadi, S. A.; Bozorgmehr, M. R. DFT-QTAIM Study of Gold Nanoparticles and Cyclic Peptide as Effective Drug Nanocarriers. *Orbital: Electron. J. Chem.* **2020**, *12*(3), 160–171.
- (13) Nasrolahi Shirazi, A.; Mandal, D.; Tiwari, R. K.; Guo, L.; Lu, W.; Parang, K. Cyclic peptide-capped gold nanoparticles as drug delivery systems. *Mol. Pharm.* **2013**, *10* (2), 500–511.



- (14) Ramadhani, D.; Maharani, R.; Gazzali, A. M.; Muchtaridi, M. Cyclic peptides for the treatment of cancers: A review. *Molecules* **2022**, *27* (14), 4428.
- (15) Tyler, T. J.; Durek, T.; Craik, D. J. Native and engineered cyclic disulfide-rich peptides as drug leads. *Molecules* **2023**, *28* (7), 3189.
- (16) Oh, D.; Darwish, S. A.; Shirazi, A. N.; Tiwari, R. K.; Parang, K. Amphiphilic bicyclic peptides as cellular delivery agents. *Chem. Med. Chem.* **2014**, *9* (11), 2449–2453.
- (17) Dougherty, P. G.; Sahni, A.; Pei, D. Understanding cell penetration of cyclic peptides. *Chem. Rev.* **2019**, *119* (17), 10241–10287.
- (18) Nasrolahi Shirazi, A.; Salem El-Sayed, N.; Kumar Tiwari, R.; Tavakoli, K.; Parang, K. Cyclic peptide containing hydrophobic and positively charged residues as a drug delivery system for curcumin. *Curr. Drug. Delv.* **2016**, *13* (3), 409–417.
- (19) Remesic, M.; Sun Lee, Y.; J Hruby, V. Cyclic opioid peptides. *Curr. Med. Chem.* **2016**, *23* (13), 1288–1303.
- (20) Martian, P. C.; Tertis, M.; Leonte, D.; Hadade, N.; Cristea, C.; Crisan, O. Cyclic peptides: A powerful instrument for advancing biomedical nanotechnologies and drug development. *J. Pharm. Biomed. Anal.* **2025**, *252*, 116488.
- (21) Ji, X.; Nielsen, A. L.; Heinis, C. Cyclic peptides for drug development. *Angew. Chem.* **2024**, *136* (3), e202308251.
- (22) Jagrosse, M. L.; Baliga, U. K.; Jones, C. W.; Russell, J. J.; García, C. I.; Najar, R. A.; Rahman, A.; Dean, D. A.; Nilsson, B. L. Impact of peptide sequence on functional siRNA delivery and gene knockdown with cyclic amphipathic peptide delivery agents. *Mol. Pharm.* **2023**, *20* (12), 6090–6103.
- (23) Hsieh, W.-H.; Liaw, J. Applications of cyclic peptide nanotubes (cPNTs). *J. F. Drug. Anal.* **2019**, *27* (1), 32–47.
- (24) Park, S. E.; Sajid, M. I.; Parang, K.; Tiwari, R. K. Cyclic cell-penetrating peptides as efficient intracellular drug delivery tools. *Mol. Pharm.* **2019**, *16* (9), 3727–3743.



- (25) Wang, C.; Shen, Z.; Chen, Y.; Wang, Y.; Zhou, X.; Chen, X.; Li, Y.; Zhang, P.; Zhang, Q. Research progress on cyclic-peptide functionalized nanoparticles for tumor-penetrating delivery. *Int. J. Nanomedicine* **2024**, 12633–12652.
- (26) Fakhari, S.; Nouri, A.; Jamzad, M.; Arab-Salmanabadi, S.; Falaki, F. Investigation of inclusion complex of metformin into selective cyclic peptides as novel drug delivery system: Structure, electronic properties, AIM, and NBO study via DFT. *J. Chin. Chem. Soc.* **2021**, 68 (1), 67–75.
- (27) Morsali, A.; Momen Heravi, M.; Beyramabadi, S. A. Selenium-capped cyclic peptide nanoparticles for penicillamine drug delivery: A DFT Study. *Indian J. Chem.-Inorg. Phys. Theor. Anal. Chem.* **2020**, 59 (1), 43–50.
- (28) Pham, D.-D.; Fattal, E.; Tsapis, N. Pulmonary drug delivery systems for tuberculosis treatment. *Int. J. Pharm.* **2015**, 478 (2), 517–529.
- (29) Chandila, S.; Kaushik, H. Current trends and challenges in tuberculosis: A systemic review. *World J. Pharm. Res.* **2023**, 12, 355–367.
- (30) Santucci, P.; Greenwood, D. J.; Fearn, A.; Chen, K.; Jiang, H.; Gutierrez, M. G. Intracellular localisation of Mycobacterium tuberculosis affects efficacy of the antibiotic pyrazinamide. *Nat. Commun.* **2021**, 12 (1), 3816.
- (31) Moumivand, A.; Naderi, F.; Moradi, O.; Makiabadi, B. Smart drug delivery: a DFT study of C24 fullerene and doped analogs for pyrazinamide. *Nanoscale. Adv.* **2025**, 7 (5), 1287–1299.
- (32) Omoteso, O. A.; Fadaka, A. O.; Walker, R. B.; Khamanga, S. M. Innovative Strategies for Combating Multidrug-Resistant Tuberculosis: Advances in Drug Delivery Systems and Treatment. *Microorganisms* **2025**, 13 (4), 722.
- (33) Clemens, D. L.; Lee, B.-Y.; Xue, M.; Thomas, C. R.; Meng, H.; Ferris, D.; Nel, A. E.; Zink, J. I.; Horwitz, M. A. Targeted intracellular delivery of antituberculosis drugs to Mycobacterium tuberculosis-infected macrophages via functionalized mesoporous silica nanoparticles. *Antimicrob. Agents Chemother.* **2012**, 56 (5), 2535–2545.



- (34) Gelperina, S.; Kisich, K.; Iseman, M. D.; Heifets, L. The potential advantages of nanoparticle drug delivery systems in chemotherapy of tuberculosis. *Am. J. Respir. Crit. Care. Med.* **2005**, *172* (12), 1487–1490.
- (35) Arnab, S. R.; Halder, J.; Islam, M. S. MoSe₂ and Al-Doped MoSe₂ as targeted carriers for anti-tuberculosis drug delivery with controlled release: A first-principles DFT study. *Inorg. Chem. Commun.* **2025**, *174*, 113979.
- (36) Sharma, A.; Sharma, S.; Khuller, G. Lectin-functionalized poly (lactide-co-glycolide) nanoparticles as oral/aerosolized antitubercular drug carriers for treatment of tuberculosis. *J. Antimicrob. Chemother.* **2004**, *54* (4), 761–766.
- (37) Rojanarat, W.; Nakpheng, T.; Thawithong, E.; Yanyium, N.; Srichana, T. Levofloxacin-proliposomes: opportunities for use in lung tuberculosis. *Pharmaceutics* **2012**, *4* (3), 385–412.
- (38) Li, C.; Wang, Y.; Zhang, X.; Deng, L.; Zhang, Y.; Chen, Z. Tumor-targeted liposomal drug delivery mediated by a diseleno bond-stabilized cyclic peptide. *Int. J. Nanomedicine.* **2013**, 1051–1062.
- (39) Buya, A. B.; Witika, B. A.; Bapolisi, A. M.; Mwila, C.; Mukubwa, G. K.; Memvanga, P. B.; Makoni, P. A.; Nkanga, C. I. Application of lipid-based nanocarriers for antitubercular drug delivery: a review. *Pharmaceutics.* **2021**, *13* (12), 2041.
- (40) Kumar, M.; Virmani, T.; Kumar, G.; Deshmukh, R.; Sharma, A.; Duarte, S.; Brandão, P.; Fonte, P. Nanocarriers in tuberculosis treatment: challenges and delivery strategies. *Pharmaceutics* **2023**, *16* (10), 1360.
- (41) Pandurangan, K.; Roy, B.; Rajasekhar, K.; Suseela, Y. V.; Nagendra, P.; Chaturvedi, A.; Satwik, U. R.; Murugan, N. A.; Ramamurthy, U.; Govindaraju, T. Molecular architectonics of cyclic dipeptide amphiphiles and their application in drug delivery. *ACS Appl. Bio Mater.* **2020**, *3* (5), 3413–3422.
- (42) Saikia, N.; Rajkhowa, S.; Deka, R. C. Density functional and molecular docking studies towards investigating the role of single-wall carbon nanotubes as nanocarrier for loading and delivery of pyrazinamide antitubercular drug onto pncA protein. *J Comput Aided Mol Des.* **2013**, *27* (3), 257



- (43) Shahabi, M.; Raissi, Heidar. Assessment of solvent effects on the inclusion behavior of pyrazinamide drug into cyclic peptide based nanotubes as novel drug delivery vehicles. *J. Mole. Liq.* **2018**, 268, 326.
- (44) Chou-Yi, H.; Mutar, A. A.; Ameer, A.J.; Kadhim, M. M.; Hamza, T. A.; ALSailawi, H.A.; Altimari, U. S.; Alawadi, Ahmed.; Alsalamy, A. Exploring boron nitride nanostructures for effective pyrazinamide drug delivery: A DFT study. *Comput. Theor. Chem.* **2023**, 1230, 114378
- (45) Frisch, M. gaussian 09, Revision d. 01, Gaussian. *Inc, Wallingford CT* **2009**, 201.
- (46) Boys, S. F.; Bernardi, F. The calculation of small molecular interactions by the differences of separate total energies. Some procedures with reduced errors. *Mol. Phys.* **1970**, 19 (4), 553–566.
- (47) Padmanabhan, J.; Parthasarathi, R.; Subramanian, V.; Chattaraj, P. Electrophilicity-based charge transfer descriptor. *J. Phys. Chem. A.* **2007**, 111 (7), 1358–1361.
- (48) Miertus, S.; Scrocco, E. Electrostatic interaction of a solute with a continuum. A direct utilizaion of AB initiomolecular potentials for the prevision of solvent effects. *J Chem Phys.* **1981**, 55, 117–129
- (49) Silvi, B.; Savin, A. Classification of chemical bonds based on topological analysis of electron localization functions. *Nature* **1994**, 371 (6499), 683–686.
- (50) Lu, T.; Chen, F. Multiwfn: A multifunctional wavefunction analyzer. *J. Comput. Chem.* **2012**, 33 (5), 580–592.
- (51) Reed, A. E.; Curtiss, L. A.; Weinhold, F. Intermolecular interactions from a natural bond orbital, donor-acceptor viewpoint. *Chem. Rev.* **1988**, 88 (6), 899–926.
- (52) Biegler-Konig, F.; Schonbohm, J.; Bayles, D. Software news and updates-AIM2000-A program to analyze and visualize atoms in molecules. *J. Comput. Chem.* **2001**, 22 (5), 545.
- (53) Ektefa, F.; Khodadadi, Z.; Naderi, F.; Fathi, F. A computational evidence of the intermolecular hydrogen bonding in leflunomide: Chemical shielding tensors. *Comput. Theor. Chem.* **2023**, 1221, 114027.



- (54) Masoodi, H. R.; Zakarianezhad, M.; Bagheri, S.; Makiabadi, B.; Shool, M. Substituent effects on some calculated NMR data in T-shaped configuration of benzene dimer. *Chem. Phys. Lett.* **2014**, *614*, 143–147.
- (55) Bagheri, S.; Masoodi, H. R.; Mohammadi, M.; Zakarianezhad, M.; Makiabadi, B. The influence of number of nitrogen atoms on the NMR data in aromatic azine... HF complexes. *Chem. Phys. Lett.* **2013**, *572*, 26–31.
- (56) Makiabadi, B.; Zakarianezhad, M.; Behjatmanesh-Ardakani, R.; Mousavi, S. H. Investigating the performance of BN nanotubes as drug delivery systems for Azacitidine and Decitabine anti-cancer drugs: A theoretical study. *Comput. Theor. Chem.* **2024**, *1231*, 114429
- (57) Hadipour, N. L.; Ahmadi Peyghan, A.; Soleymanabadi, H. Theoretical study on the Al-doped ZnO nanoclusters for CO chemical sensors. *J. Phys. Chem. C.* **2015**, *119* (11), 6398.
- (58) Zhu, H.; Zhao, C.; Cai, Q.; Fu, X.; Sheykhahmad, F. R. Adsorption behavior of 5-aminosalicylic acid drug on the B₁₂N₁₂, AlB₁₁N₁₂ and GaB₁₁N₁₂ nanoclusters: A comparative DFT study. *Inorg. Chem. Commun.* **2020**, *114*, 107808.
- (59) Johnson, E. R.; Keinan, S.; Mori-Sánchez, P.; Contreras-García, J.; Cohen, A. J.; Yang, W. Revealing noncovalent interactions. *J. Am. Chem. Soc.* **2010**, *132* (18), 6498–6506.



Data Availability Statement

The datasets generated and analyzed during the current study are available from the corresponding author upon reasonable request.

